

Green $\text{SrSi}_2\text{O}_2\text{N}_2\text{:Eu}^{2+}$ phosphor for LED-phosphor applications: synthesis and characterization

Ha Thanh Tung¹, My Hanh Nguyen Thi²

¹Faculty of Basic Sciences, Vinh Long University of Technology Education, Vinh Long Province, Vietnam

²Faculty of Mechanical Engineering, Industrial University of Ho Chi Minh City, Ho Chi Minh City, Vietnam

Article Info

Article history:

Received Oct 27, 2022

Revised Nov 2, 2022

Accepted Jan 11, 2023

Keywords:

Color homogeneity

Double-layer phosphor

Luminous flux

$\text{SrSi}_2\text{O}_2\text{N}_2\text{:Eu}^{2+}$

WLEDs

ABSTRACT

Green phosphors $\text{SrSi}_2\text{O}_2\text{N}_2\text{:Eu}^{2+}$ (SSON:Eu) are combined utilizing a simple solid-state reaction with $\text{SrSi}_2\text{O}_2\text{N}_2\text{:Eu}^{2+}$ like the forerunner. Various phosphor attributes were assessed following creation procedure. Differential thermal analysis (DTA) spectra and luminescence measurements are used to assess crystalline active power, electron-phonon conjunction, and heat quenching behavior. Because of their poor electron-phonon conjunction intensity (Huang-Rhys factor=4.2), SSON:Eu green phosphors have outstanding heating and color consistency. The heat quenching temperature (T_{50}) of SSON:Eu is greater than 200 °C. SSON:Eu green phosphors have a wide stimulation range, strong heat steadiness and can absorb ultraviolet (UV) to blue energy and release green illumination, leading to the appropriate utilization in solid-state illumination and GaAsAl solar cells, according to the findings.

This is an open access article under the [CC BY-SA](https://creativecommons.org/licenses/by-sa/4.0/) license.



Corresponding Author:

My Hanh Nguyen Thi

Faculty of Mechanical Engineering, Industrial University of Ho Chi Minh City

Ho Chi Minh City, Vietnam

Email: nguyenthimyanh@iuh.edu.vn

1. INTRODUCTION

Phosphors are commonly employed in high-performance implementations such as phosphor-transformed illumination-releasing diodes light-emitting diodes (LEDs), liquid crystal display backlights, and solar-cell panels [1], [2]. Since they imbibe close-ultraviolet (UV) or blue illumination (380–470 nm) from LEDs and generate sufficient viewable illumination in regularly utilized sulfide, silicate, or oxynitride/nitride host substances, Eu^{2+} -doped phosphors are widely utilized in LEDs [3], [4]. As a result, transformation phosphors must have a broad stimulation band that encompasses this range of wavelength. Oxynitride phosphors, like Ca-SiAlON:Eu^{2+} , SSON:Eu, and $\text{CaSi}_2\text{O}_2\text{N}_2\text{:Eu}^{2+}$, have lately received much interest because they have great chemical steadiness and no toxicity [5]. They have substantial absorptivity between the close-UV and blue illumination spectrum, which exactly matches the supplied illumination of mercantile LEDs, helping them to be suitable choices for white LEDs (WLED's). Nevertheless, the synthesizing requirements for oxynitride-based phosphors are extremely stringent, necessitating elevated temperatures and elevated N_2 tension. According to this paper, a normal-pressure sintering process is offered to produce SSON:Eu phosphors from $\text{Sr}_2\text{SiO}_4\text{:Eu}^{2+}$ like a forerunner. Computing the activation energy of crystallization yields the reaction mechanism. SSON:Eu phosphors have earlier been examined, however just the luminescence and configuration characteristics were described [6], [7]. Research by Durmus and Davis [8] found that the heat quenching temperature of SSON:Eu is around 600 K. (327 °C). Low crystallization activating energy for substance synthesizing methods suggests that the synthesizing technique is straightforward to conduct [9], [10]; also the compounds having great crystallization may be

generated. Phosphors having high crystallization will also include a high luminosity. As a result, we can utilize the crystallization activation energy to specify the best combination technique. In [11] and [12] found the crystallized activating power of glass ceramics with silicate/oxy-nitride base around ~400 and 834 kJ/mol, correspondingly, utilizing a distinctive heating study differential thermal analysis (DTA). The SSON:Eu phosphors' crystallized activating power are determined in this study. Also explored are the electron-phonon linking intensity, heat steadiness, and hue consistency of SSON:Eu phosphors. Further data on the phosphor samples will be discussed in sections 2 and 3 which concern the computation of phosphor attributes and the assessment of phosphor influence on WLED's factors. The findings demonstrate that the phosphors' wide band-type stimulation and emission are ideal for solid-state illumination and solar cell uses, as shown in sections 4.

2. COMPUTATIONAL SIMULATION

SSON:Eu specimens were produced in a one-stage and two-stage solid-state synthesis, accordingly. For the sole-stage combination technique (I) (specimen I), the initial substances, having 99.9% purity, includes SrCO_3 , SiO_2 , Eu_2O_3 , and $\alpha\text{-Si}_3\text{N}_4$. We combine them by pulverizing and sintering in one horizontal pipe furnace under 1,450 °C within 6 hours below decreasing environment (5% H_2 –95% N_2). A combination including SrCO_3 , SiO_2 , and Eu_2O_3 was burned underneath a decreasing environment at 1250 °C within 3 hours for creating $\text{Sr}_2\text{SiO}_4\text{:Eu}^{2+}$ specimens for the two-stage synthesis method (II) (specimen II). The $\text{SrSiO}_4\text{:Eu}^{2+}$ specimen and Si_3N_4 combination were then burned once more at 1,450 °C for 6 hours within the similar decreasing environment for obtaining SSON:Eu phosphors [13], [14].

One of the most commonly utilized techniques in crystallization kinetic investigations is the Kissinger technique. We utilize the Kissinger equation to calculate the crystallized activating power [15]:

$$\ln(\Phi/T_p^2) = \frac{-E_c}{RT_p} + c \quad (c=\text{constant}) \quad (1)$$

Where Φ denotes the DTA scan ratio (°C/min), T_p denotes the highest DTA crystallized highest heat (K), and $R=8.3144 \text{ J/mol K}$ and represents the gas constant. E_c represents the crystallized activating power, calculated relying to the slope of the $\ln(\Phi/T_p^2)$ vs. $10^3/RT_p$ plot. The temperature dependence of luminous strength can be described using the Arrhenius [15]:

$$I(T) = \frac{I_0}{\left[1 + C \exp\left(\frac{-\Delta E}{kT}\right)\right]} \quad (2)$$

A and C represent constant factors, k represents Boltzmann's constant, I_0 demotes the starting strength, $I(T)$ denotes the strength at the provided heat T, and ΔE denotes the activating power for the heat extinguishing phase, calculated according to the incline for $\ln[(I_0/I(T))-1]$ vs. $1/kT$ plot. A smaller ΔE scope indicates a faster non-radiation ratio with a provided heat. The emission spectra's full width half maximum (FWHM) (T) can be explained through utilizing the configurational coordinate design as well as Boltzmann [16] dispensation as:

$$FWHM(T) = hv[8 \times \ln 2 \times S \times \coth(hv/2k_B T)]^{1/2} \quad (3)$$

Where hv represents the medium phonon power. S represents the Huang-Rhys number. k_B represents the Boltzmann constant. The electron-phonon coupling strength is represented by the Huang-Rhys parameter S. If $S < 1$, the linking is faint; if $1 < S < 5$, the coupling is mean; and if $S > 5$, the coupling is potent. Dorenbos [17] defined this relationship as (4):

$$FWHM(T) = hv[8 \times \ln 2 \times S \times \coth(hv/2k_B T)]^{1/2} \quad (4)$$

Where $E_{\text{free}}=4.19 \text{ eV}$ and represents the power variation regarding gaseous-state Eu^{2+} ions, and D denotes the redshift power reduction.

3. RESULTS AND DISCUSSION

The demand for stable and effective phosphors in the red region of the emission spectrum, which oxides cannot easily offer, stimulated research in various phosphor base types having a large crystal field and/or a big centroid shift. It is obvious that the extensive-band emitting rare-earth ions like Eu^{2+} as well as Ce^{3+} have virtually optimal characteristics; the remaining issue is to identify acceptable hosts with a large enough redshift. This property was discovered in (oxy)nitride phosphors, prompting a significant investigation into this novel class of materials throughout the last decade. Generally, (oxy)nitride phosphors have outweighed other phosphors in terms of thermal and chemical stabilities. They were also studied for

their outstanding thermal and chemical stability, strength, and hardness, making them appropriate for abrasives and protective coatings. Nevertheless, previous studies did not examine much about their luminescent characteristics. Additionally, the stability examinations for oxidation or the photo-thermal influence of LED's large fluxes were barely reported. The next section will demonstrate the influence simulation of SSON:Eu on the WLED luminescence and color characteristics.

Figure 1 illustrates the inverse variation for SSON:Eu as well as YAG:Ce³⁺ phosphor presence regarding three correlated color temperature (CCT) of 3,000 K (Figure 1(a)), 4,000 K (Figure 1(b)), and 5,000 K (Figure 1(c)). Two implications are made by such shift: the first is to keep mean CCTs stable, and the second is to impact absorbance and dispersion in the phosphor-layer structure of WLEDs. As light absorbance and dispersion are impacted, the chroma adequacy along with luminous flux in the WLED apparatus are also modified. As such, the SSON:Eu concentration alters the color quality of WLEDs. The YAG:Ce³⁺ concentration dropped as the SSON:Eu concentration climbed from 2 to 20% by weight for preserving the average CCTs (5,600-8,500 K) [18].

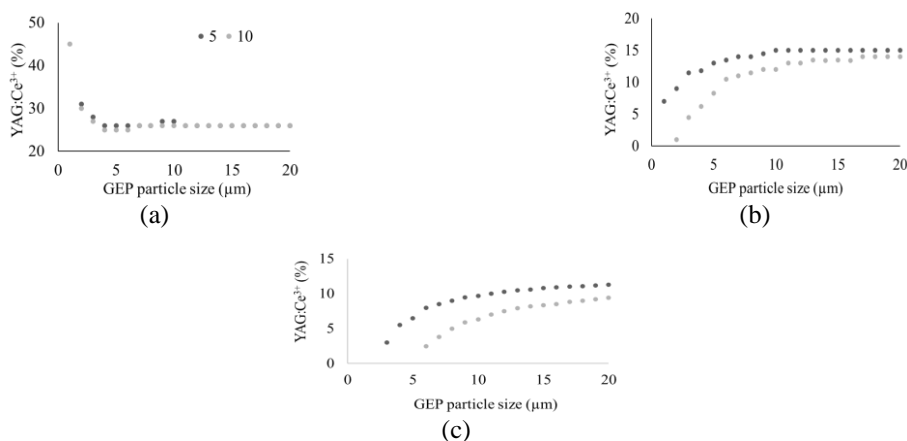


Figure 1. Varying concentrations for phosphors to retain the stable CCT (a) 3,000 K, (b) 4,000 K, and (c) 5,000 K

Figure 2 shows the SSON:Eu presence's impact on the WLED's transmitting spectra observed at 3,000 K (Figure 2(a)), 4,000 K (Figure 2(b)), and 5,000 K (Figure 2(c)). By observing the change in the strength of emission in certain wavelengths, in connection with the change in green phosphor concentration, we can possibly find out the suitable to obtain high lumen for WLEDs [19], [20]. As shown in the data, the emission bands are obvious in 420-480 nm along with 500-640 nm wavelength zones. Moreover, the peaks in these two emission wavelength bands are at ~420 and ~505 nm, meaning that the blue and green emissions are stronger. This benefits the luminance power of the WLED. So, it means that SSON:Eu could notably improve emissions strengths or luminescence of the white light from LEDs. The results in Figure 3 are used to re-confirm the enhancement in the luminosity of WLEDs when applying the SSON:Eu phosphor. At all three CCTs, 3,000 K (Figure 3(a)), 4,000 K (Figure 3(b)), and 5,000 K (Figure 3(c)), the luminous flux emitted grows dramatically when the SSON:Eu proportion grows in the range 2-20% wt.

Besides the luminosity, the angular divergence on the chroma scale was dramatically reduced with the phosphor SSON:Eu proportion in three average CCTs, based on the results in Figure 4, exhibiting CCT levels of 3,000 K (Figure 4(a)), 4,000 K (Figure 4(b)), and 5,000 K (Figure 4(c)). This is because of the enhanced dispersion of blue illumination and the absorptivity of the green-phosphor SSON:Eu. When phosphor SSON:Eu was integrated, blue emission was enhanced (see Figures 2(a)-(c)), improving the probability of blue-light scattering and dispersing inside the WLED structure. Then, every time the blue light encounters the green phosphor particle, it is absorbed easily. The green phosphor subsequently emits the green illumination through the down-conversion process. Though the yellow light is absorbed by SSON:Eu granules, it is just a smaller amount, compared to that of the blue light. With the enhanced dispersion and supplemented green light, the color divergence is reduced for the enhancement of color uniformity [21], [22]. Obviously, color uniformity is an important feature of high-quality WLED, and so does the luminosity. Thus, the concentration of SSON:Eu should be selected based on the application requirements, whether it requires to have high-color-quality WLED or high-luminescence WLED. The WLED with high color quality could emit a relatively weaker luminescence. Besides, the better the chromatic consistency index, the more costly the WLED. Employing SSON:Eu only requires an inexpensive cost. SSON:Eu can therefore be broadly used.

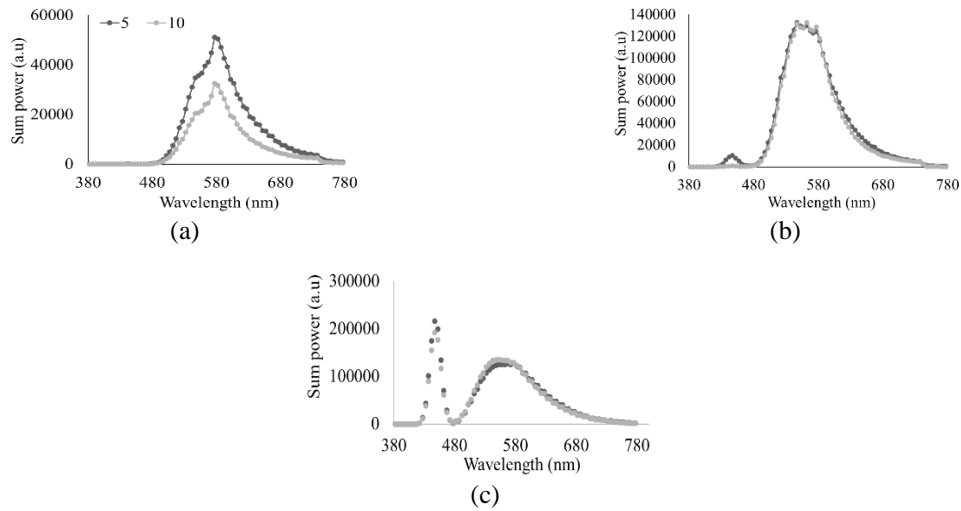


Figure 2. Intensities of WLEDs' emission bands correlating with SSON:Eu presence: (a) 3,000 K, (b) 4,000 K, and (c) 5,000 K

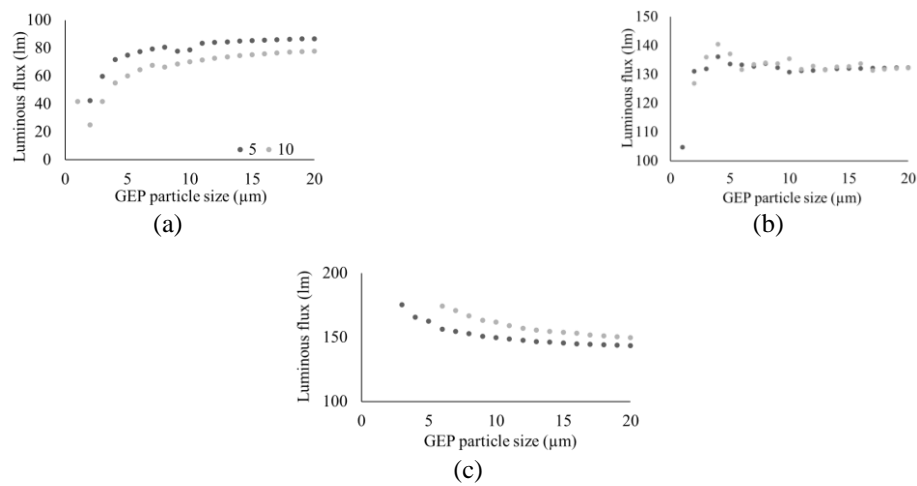


Figure 3. The optical flux from WLED responding to SSON:Eu presence (a) 3,000 K, (b) 4,000 K and (c) 5,000 K

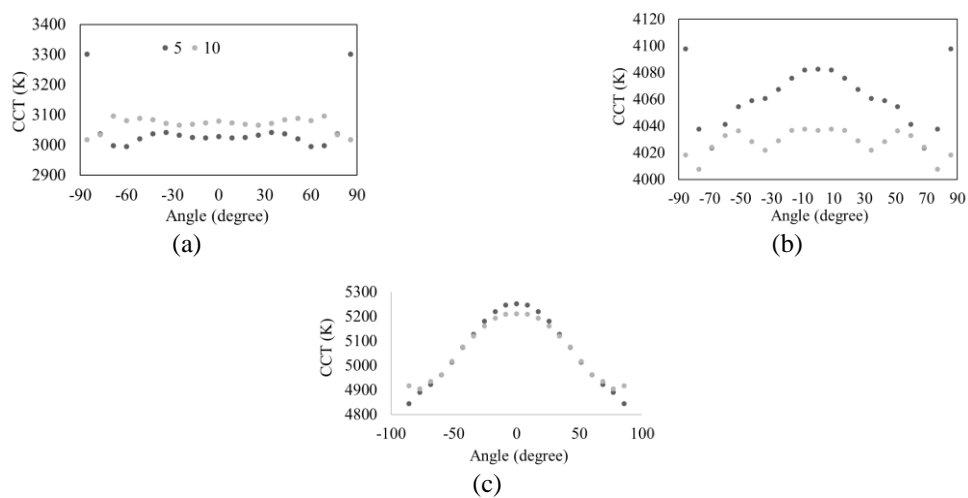


Figure 4. WLED's CCT correlating with SSON:Eu presence: (a) 3,000 K, (b) 4,000 K, and (c) 5,000 K

Hue quality cannot be claimed to be good when having only a good hue homogeneity indicator. It needs to consider other two factors, consisting of color rendition intent (CRI) and the preference of viewers' visuality [23], [24]. Researchers have developed and used the color quality scale (CQS) to access these three important factors. The CRI is used to evaluate the real hue of a lightened object revealed by a tested light. The data recorded for CRI and CQS were shown in Figures 5 and 6. At all CCTs 3,000-5,000K (Figures 5(a)-(c)), CRI showed a small reduction when accompanied by a SSON:Eu sheet. In Figures 6(a)-(c), it is possible to observe how CQS is amplified when accompanied by the SSON:Eu film. On the other hand, if SSON:Eu concentrations are below 10% wt, CQS is hardly altered. If SSON:Eu concentrations are above 10% wt., CQS and also CRI significantly reduced because of severe hue imbalance when green is dominant over the other two main hues, blue and yellow [25]–[28]. WLED color accuracy is reduced as a result of this having an effect on the hue standard of WLEDs. Owing to that, an appropriate choice on SSON:Eu weight percentage is very necessary.

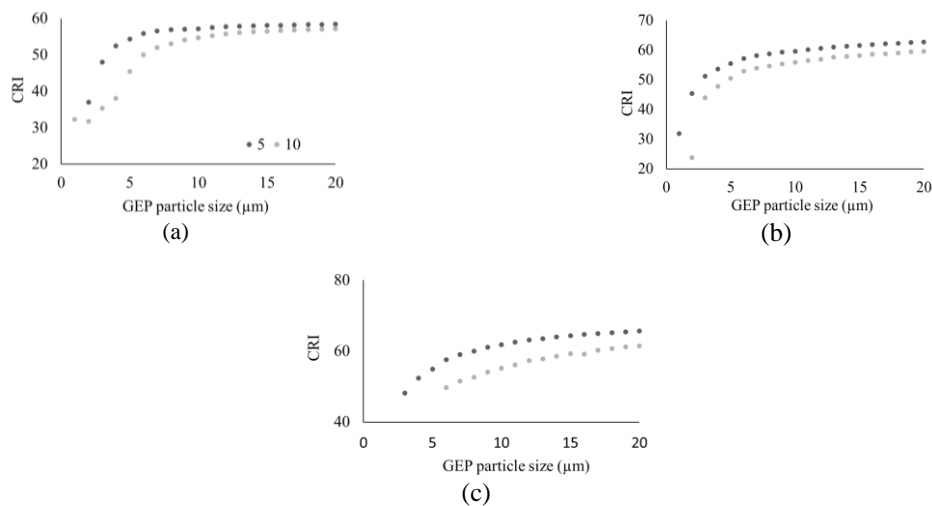


Figure 5. CRI in WLED device correlating with SSON:Eu presence (a) 3,000 K; (b) 4,000 K, and (c) 5,000 K

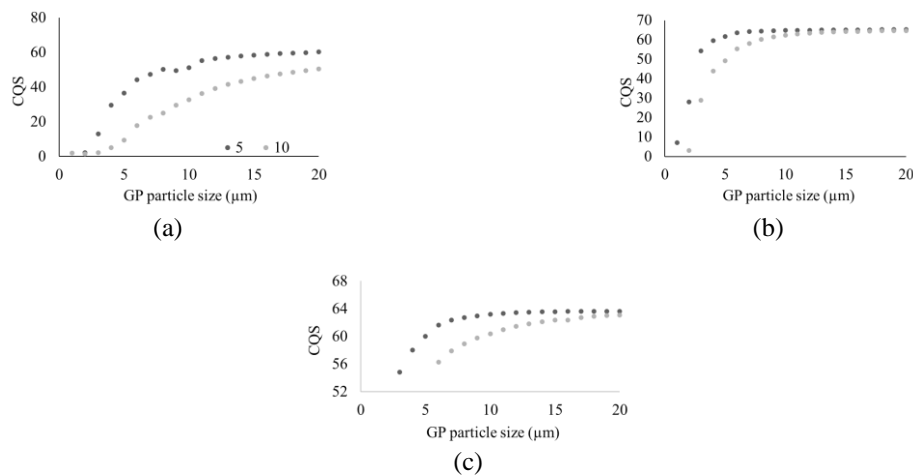


Figure 6. CQS in WLED device correlating with SSON:Eu presence (a) 3,000 K, (b) 4,000 K, and (c) 5,000 K

4. CONCLUSION




Green phosphors SSON:Eu produced from $\text{Sr}_2\text{SiO}_4\text{:Eu}^{2+}$ exhibit small crystallized activating power (408.82 KJ/mol) and a low Huang-Rhys number (4.2). SSON:Eu has a heat quenching temperature (T_{50}) more than 200 °C. Because of their poor electron-phonon coupling strength, SSON:Eu demonstrates remarkable temperature and color stability. SSON:Eu phosphors absorb UV to blue energy and release green

illumination, potentially improving the GaAsAl solar cells' effectiveness. The findings suggest SSON:Eu green phosphors could be used in solid-state illumination and solar cells.




REFERENCES

- [1] X. Tao *et al.*, "Performance enhancement of yellow InGaN-based multiple-quantum-well light-emitting diodes grown on Si substrates by optimizing the InGaN/GaN superlattice interlayer," *Optical Materials Express*, vol. 8, no. 5, pp. 1221–1230, May 2018, doi: 10.1364/OME.8.001221.
- [2] K. H. Li *et al.*, "Monolithically integrated InGaN/GaN light-emitting diodes, photodetectors, and waveguides on Si substrate," *Optica*, vol. 5, no. 5, pp. 564–569, May 2018, doi: 10.1364/OPTICA.5.000564.
- [3] C. F. Fong *et al.*, "Silicon nitride nanobeam enhanced emission from all-inorganic perovskite nanocrystals," *Optics Express*, vol. 27, no. 13, pp. 18673–18682, Jun. 2019, doi: 10.1364/OE.27.018673.
- [4] V. Ryzhii *et al.*, "Theoretical analysis of injection driven thermal light emitters based on graphene encapsulated by hexagonal boron nitride," *Optical Materials Express*, vol. 11, no. 2, pp. 468–486, Feb. 2021, doi: 10.1364/OME.412973.
- [5] P. S. Yeh, Y.-C. Chiu, T.-C. Wu, Y.-X. Chen, T.-H. Wang, and T.-C. Chou, "Monolithic integration of GaN-based phototransistors and light-emitting diodes," *Optics Express*, vol. 27, no. 21, pp. 29854–29862, Oct. 2019, doi: 10.1364/OE.27.029854.
- [6] B. Jain, R. T. Velpula, M. Patel, and H. P. T. Nguyen, "Controlled carrier mean free path for the enhanced efficiency of III-nitride deep-ultraviolet light-emitting diodes," *Applied Optics*, vol. 60, no. 11, pp. 3088–3093, Apr. 2021, doi: 10.1364/AO.418603.
- [7] N. K. Manjunath, Y. Lu, and S. Lin, "Van der Waals contacted MoO_x staked ZnO/GaN vertical heterostructured ultraviolet light emitting diodes," *Optics Express*, vol. 28, no. 21, pp. 31603–31610, Oct. 2020, doi: 10.1364/OE.402261.
- [8] D. Durmus and W. Davis, "Blur perception and visual clarity in light projection systems," *Optics Express*, vol. 27, no. 4, pp. 216–223, Feb. 2019, doi: 10.1364/OE.27.00A216.
- [9] W. Bao, M. Wei, and K. Xiao, "Investigating unique hues at different chroma levels with a smaller hue angle step," *Journal of the Optical Society of America A*, vol. 37, no. 4, pp. 671–679, Apr. 2020, doi: 10.1364/JOSAA.383002.
- [10] H. Jiang *et al.*, "Projection optical engine design based on tri-color LEDs and digital light processing technology," *Applied Optics*, vol. 60, no. 23, pp. 6971–6977, Aug. 2021, doi: 10.1364/AO.432355.
- [11] Z. Zhao, H. Zhang, S. Liu, and X. Wang, "Effective freeform TIR lens designed for LEDs with high angular color uniformity," *Applied Optics*, vol. 57, no. 15, pp. 4216–4221, May 2018, doi: 10.1364/AO.57.004216.
- [12] I. G. Palchikova, E. S. Smirnov, and E. I. Palchikov, "Quantization noise as a determinant for color thresholds in machine vision," *Journal of the Optical Society of America A*, vol. 35, no. 4, pp. 214–222, Apr. 2018, doi: 10.1364/JOSAA.35.00B214.
- [13] S. K. Abeysekera, V. Kalavally, M. Ooi, and Y. C. Kuang, "Impact of circadian tuning on the illuminance and color uniformity of a multichannel luminaire with spatially optimized LED placement," *Optics Express*, vol. 28, no. 1, pp. 130–145, Jan. 2020, doi: 10.1364/OE.381115.
- [14] L. V. Labunets, A. B. Borzov, and I. M. Akhmetov, "Regularized parametric model of the angular distribution of the brightness factor of a rough surface," *Journal of Optical Technology*, vol. 86, no. 10, pp. 618–626, Oct. 2019, doi: 10.1364/JOT.86.000618.
- [15] Y. Tang, Z. Li, G. Liang, Z. Li, J. Li, and B. Yu, "Enhancement of luminous efficacy for LED lamps by introducing polyacrylonitrile electrospinning nanofiber film," *Optics Express*, vol. 26, no. 21, pp. 27716–27725, Oct. 2018, doi: 10.1364/OE.26.027716.
- [16] X. Ding *et al.*, "Improving the optical performance of multi-chip LEDs by using patterned phosphor configurations," *Optics Express*, vol. 26, no. 6, pp. 283–292, Mar. 2018, doi: 10.1364/OE.26.00A283.
- [17] M. J. Egan, A. Colón, S. M. Angel, and S. Sharma, "Suppressing the multiplex disadvantage in photon-noise limited interferometry using cross-dispersed spatial heterodyne spectrometry," *Applied Spectroscopy*, vol. 75, no. 2, pp. 208–215, Jul. 2020, doi: 10.1177/0003702820946739.
- [18] H. Daicho, K. Enomoto, H. Sawa, S. Matsuishi, and H. Hosono, "Improved color uniformity in white light-emitting diodes using newly developed phosphors," *Optics Express*, vol. 26, no. 19, pp. 24784–24791, Sep. 2018, doi: 10.1364/OE.26.024784.
- [19] N. C. Abd Rashid *et al.*, "Spectrophotometer with enhanced sensitivity for uric acid detection," *Chinese Optics Letters*, vol. 17, no. 8, pp. 1–5, 2019, doi: 10.3788/COL201917.081701.
- [20] M. J. H. Anthonissen, L. B. Romijn, J. H. M. T. T. Boonkamp, and W. L. IJzerman, "Unified mathematical framework for a class of fundamental freeform optical systems," *Optics Express*, vol. 29, no. 20, pp. 31650–31664, Sep. 2021, doi: 10.1364/OE.438920.
- [21] A. A. Pan'kov, "Informative light pulses of indicating polymer fiber-optic piezoelectroluminescent coatings upon indentation of rigid globular particles," *Journal of Optical Technology*, vol. 88, no. 8, pp. 477–482, Aug. 2021, doi: 10.1364/JOT.88.000477.
- [22] J. X. Yang, D. S. Li, G. Li, E. Y. B. Pun, and H. Lin, "Photon quantification in Ho³⁺/Yb³⁺ co-doped opto-thermal sensitive fluorotellurite glass phosphor," *Applied Optics*, vol. 59, no. 19, pp. 5752–5763, Jul. 2020, doi: 10.1364/AO.396393.
- [23] J. Hao, H.-L. Ke, L. Jing, Q. Sun, and R.-T. Sun, "Prediction of lifetime by lumen degradation and color shift for LED lamps, in a non-accelerated reliability test over 20,000 h," *Applied Optics*, vol. 58, no. 7, pp. 1855–1861, Mar. 2019, doi: 10.1364/AO.58.001855.
- [24] A. K. Dubey, M. Gupta, V. Kumar, and D. S. Mehta, "Laser-line-driven phosphor-converted extended white light source with uniform illumination," *Applied Optics*, vol. 58, no. 9, pp. 2402–2407, Mar. 2019, doi: 10.1364/AO.58.002402.
- [25] S. An, J. Zhang, and L. Zhao, "Optical thermometry based on upconversion luminescence of Yb³⁺-Er³⁺ and Yb³⁺-Ho³⁺ doped Y₆WO₁₂ phosphors," *Applied Optics*, vol. 58, no. 27, pp. 7451–7457, Sep. 2019, doi: 10.1364/AO.58.007451.
- [26] T. DeLawyer, M. Tayon, C. Yu, and S. L. Buck, "Contrast-dependent red-green balance shifts depend on S-cone activity," *Journal of the Optical Society of America A*, vol. 35, no. 4, pp. 114–121, Apr. 2018, doi: 10.1364/JOSAA.35.00B114.
- [27] W. Gao, K. Ding, G. He, and P. Zhong, "Color temperature tunable phosphor-coated white LEDs with excellent photometric and colorimetric performances," *Applied Optics*, vol. 57, no. 31, pp. 9322–9327, Nov. 2018, doi: 10.1364/AO.57.009322.
- [28] V. M. Igba *et al.*, "Structural elucidation and optical properties of LiZrO₂-LiBaZrO₃ nanocomposite doped with Mn²⁺ ions," *Optical Materials Express*, vol. 10, no. 11, pp. 2877–2895, Nov. 2020, doi: 10.1364/OME.402111.

BIOGRAPHIES OF AUTHORS

Ha Thanh Tung    received the Ph.D. degree in physics from University of Science, Vietnam National University Ho Chi Minh City, Vietnam, he is working as a lecturer at the Faculty of Basic Sciences, Vinh Long University of Technology Education, Vietnam. His research interests focus on developing the patterned substrate with micro-and nano-scale to apply for physical and chemical devices such as solar cells, OLED, and photoanode. He can be contacted at email: tunght@vlute.edu.vn.



My Hanh Nguyen Thi    received a Bachelor of Physics from An Giang University, VietNam, Master of Theoretical Physics and Mathematical Physics, Hanoi National University of Education, Vietnam. Currently, she is a lecturer at the Faculty of Mechanical Engineering, Industrial University of Ho Chi Minh City, Vietnam. Her research interests are theoretical physics and mathematical physics. She can be contacted at email: nguyenthimyanh@iuh.edu.vn.